

# Lens Epithelial Cells Initiate an Inflammatory Response Following Cataract Surgery

Jian Jiang,<sup>1,2</sup> Mahbubul H. Shihan,<sup>2</sup> Yan Wang,<sup>2</sup> and Melinda K. Duncan<sup>2</sup>

<sup>1</sup>Department of Ophthalmology, Xiangya Hospital, Central South University, Changsha, Hunan, China

<sup>2</sup>Department of Biological Sciences, University of Delaware, Newark, Delaware, United States

Correspondence: Melinda K. Duncan, Department of Biological Sciences, University of Delaware, Newark, DE 19716, USA; duncanm@udel.edu.

JJ and MHS contributed equally to the work presented here and should therefore be regarded as equivalent authors.

Submitted: June 15, 2018

Accepted: August 21, 2018

Citation: Jiang J, Shihan MH, Wang Y, Duncan MK. Lens epithelial cells initiate an inflammatory response following cataract surgery. *Invest Ophthalmol Vis Sci.* 2018;59:4986-4997. <https://doi.org/10.1167/iov.18-25067>

**PURPOSE.** Lens epithelial cell (LEC) conversion to myofibroblast is responsible for fibrotic cataract surgery complications including posterior capsular opacification. While transforming growth factor beta (TGF $\beta$ ) signaling is important, the mechanisms by which the TGF $\beta$  pathway is activated post cataract surgery (PCS) are not well understood.

**METHODS.** RNA-seq was performed on LECs obtained from a mouse cataract surgery model at the time of surgery and 24 hours later. Bioinformatic analysis was performed with iPathwayGuide. Expression dynamics were determined by immunofluorescence.

**RESULTS.** The LEC transcriptome is massively altered by 24 hours PCS. The differentially expressed genes included those important for lens biology, and fibrotic markers. However, the most dramatic changes were in the expression of genes regulating the innate immune response, with the top three altered genes exhibiting greater than 1000-fold upregulation. Immunolocalization revealed that CXCL1, S100a9, CSF3, COX-2, CCL2, LCN2, and HMOX1 protein levels upregulate in LECs between 1 hour and 6 hours PCS and peak at 24 hours PCS, while their levels sharply attenuate by 3 days PCS. This massive upregulation of known inflammatory mediators precedes the infiltration of neutrophils into the eye at 18 hours PCS, the upregulation of canonical TGF $\beta$  signaling at 48 hours PCS, and the infiltration of macrophages at 3 days PCS.

**CONCLUSIONS.** These data demonstrate that LECs produce proinflammatory cytokines immediately following lens injury that could drive postsurgical flare, and suggest that inflammation may be a major player in the onset of lens-associated fibrotic disease PCS.

**Keywords:** posterior capsular opacification, inflammation, fibrosis, cataract surgery, lens epithelial cell

Cataracts have traditionally been the most prevalent cause of human blindness; however, in recent decades, their impact has been greatly reduced by the adoption of extracapsular and/or phacoemulsification cataract extraction followed by intraocular lens (IOL) implantation into the lens capsular bag.<sup>1-4</sup> However, the long-term outcome of cataract surgery is compromised when residual lens epithelial cells (LECs) begin proliferating concurrently with either epithelial-mesenchymal transition (EMT) leading to the formation of profibrotic myofibroblasts, or the onset of a regenerative response where the remnant LECs convert to structurally aberrant lens fibers.<sup>5</sup> If these LEC-derived cells remain at the periphery, they form Soemmering's ring, which is largely benign<sup>6</sup> or even beneficial for long-term IOL stability.<sup>7</sup> However, Soemmering's ring can continue to expand many years post cataract surgery (PCS), compromising the function of advanced IOLs,<sup>8,9</sup> even leading to late IOL dislocation.<sup>10</sup> If LEC-derived myofibroblasts migrate anteriorly PCS, they can cause anterior capsular fibrosis/phimosi, which opacifies the visual axis and can decentrate the IOL.<sup>11,12</sup> If myofibroblasts migrate onto the posterior lens capsule, they again form scar tissue in the visual axis leading to fibrotic posterior capsular opacification (PCO).<sup>13,14</sup> Finally, even if the posterior lens capsule is ablated at the time of surgery, lens-derived myofibroblasts can opacify the visual axis

by migrating from the lens capsular bag onto the anterior hyaloid membrane, particularly in pediatric patients.<sup>15,16</sup>

While there is controversy in the literature about the population-wide rates of these undesirable outcomes, PCO rates alone are reported to be 40% or higher in adult patients living 10 years or more PCS,<sup>14,17</sup> and approach 100% in children.<sup>15,16</sup> While these PCS side effects are generally treatable by either YAG laser ablation or surgery, poor outcomes can result due to ocular inflammation, difficulties ablating dense fibrosis, IOL displacement, and retinal complications.<sup>18-21</sup> Thus, prevention of LEC EMT would improve the long-term visual outcome of cataract surgery.<sup>14,19</sup>

Transforming growth factor beta (TGF $\beta$ ) signaling can drive LEC EMT,<sup>22</sup> while sustained TGF $\beta$  signaling has been observed in both fibrotic PCO<sup>23</sup> and the lens fibrotic disease, anterior subcapsular cataract (ASC).<sup>24,25</sup> However, while TGF $\beta$  concentrations are high in the eye even prior to surgery, most of this TGF $\beta$  is in an inactive form<sup>26</sup> and is thus unable to elicit fibrotic responses. This makes it likely that the induction of pathways that result in latent TGF $\beta$  activation<sup>27-30</sup> are key steps in PCO pathogenesis.

We developed an in vivo mouse model of cataract surgery where the lens fiber cells are surgically removed, leaving behind the lens capsule and attached LECs.<sup>31,32</sup> In this model, the upregulation of mRNAs encoding fibrotic markers such as  $\alpha$ -

smooth muscle actin ( $\alpha$ -SMA), fibronectin, and tenascin-C are detected in remnant LECs 24 hours PCS, while the first induction of these proteins is seen 48 hours PCS.<sup>33</sup> Notably, though, it takes 48 hours for the first obvious upregulation of the pSMAD2/3 levels associated with TGF $\beta$  pathway activation, and up to 5 days for a maximal response.<sup>33</sup> This lag between injury and TGF $\beta$  pathway activation thus makes the mouse an excellent model to study the mechanisms by which ocular trauma/surgery results in fibrotic PCO, and we have successfully used this mouse “cataract surgery” model to direct the power of mouse genetics to the study of PCO pathogenesis.<sup>32,33</sup> Here we use RNA-seq to discover the gene expression changes that LECs undergo after cataract surgery but prior to the onset of TGF $\beta$  signaling. This analysis revealed that LECs robustly activate the innate immune response within hours of cataract surgery and supports prior speculation that postsurgical inflammation is mechanistically related to lens capsular bag fibrosis PCS.<sup>34</sup>

## METHODS

### Animals

All animals used in this study were treated in accordance with the ARVO Statement for the Use of Animals in Ophthalmic and Vision Research and were approved by the University of Delaware Institutional Animal Care and Use Committee under protocol 1039. Mice were either obtained from Envigo/Harlan Sprague-Dawley (C57BL/6NHsd; Indianapolis, IN, USA) or were bred in house. All mice were maintained under pathogen-free conditions at the University of Delaware animal facility under a 14/10-hour light/dark cycle.

### Lens Injury/Cataract Surgery Model

This animal model for PCO development has been described previously.<sup>31–33</sup> Mice at 10 to 16 weeks old were anesthetized with ketamine/xylazine and the pupil of one eye was dilated with 1% tropicamide and 2.5% phenylephrine hydrochloride ophthalmic solution (Akorn, Lake Forest, IL, USA). A 3-mm central corneal incision extending into the lens capsule was made with an ophthalmic knife. The lens fiber mass was separated from the lens capsule by hydrodissection with balanced salt solution, mechanically split in two, and removed from the eye. The corneal incision was closed with 10-0 nylon suture and the anterior chamber was refilled with balanced salt solution. Mice were allowed to recover for the desired time following surgery to allow for LEC responses. Mice were then again anesthetized, and the other eye was subjected to lens fiber cell removal; they were immediately killed so that the contralateral eye could serve as a time zero control. The eyes were then harvested, and processed for further analysis.

### RNA Sequencing

The lens fiber cells were removed from one eye of C57BL/6NHsd mice and 24 hours later, the other eye was operated on to create a time zero control, followed by immediate euthanasia. Lens capsular bags with attached cells were isolated, and samples from five individual mice were pooled, and flash frozen on dry ice to create one 0-hour and one 24-hour PCS biological replicate. RNA was isolated using the RNeasy Mini Kit (50) from Qiagen (Cat. No./ID: 74104; Germantown, MD, USA). One microgram total RNA was processed using the Illumina TruSeq RNA Sample Prep Kit (Cat#FC-122-1001; San Diego, CA, USA) to produce sequencing libraries, which were analyzed on an Illumina HiSeq 2500 by the Genotyping and Sequencing Center, Delaware Biotechnology Institute, University of Delaware.

Sequence data were analyzed against the *Mus musculus* mm10 genome build (UCSC tophat version as downloaded May 2017) by the University of Delaware Bioinformatics Core Facility using a modified MAP-Rseq pipeline<sup>35</sup> implemented on the BioMix computer cluster at the Center for Bioinformatics and Computational Biology/Delaware Biotechnology Institute. Pairwise differential expression analysis was performed on features with >1 counts per million (cpm) in at least two samples and statistically analyzed using the pairwise quintile-adjusted conditional maximum likelihood method exact test with a Benjamini Hochberg false discovery rate (FDR) correction run on the EdgeR BioConductor package v 3.16.5.<sup>36</sup> Biologically significant differentially expressed genes (DEGs) are defined as previously described as those exhibiting statistically significant changes (FDR  $\leq$  0.05) in level between 0 and 24 hours PCS, a change in mRNA level greater than 2 reads per kilobase per million (RPKM), a fold change (FC)  $\geq$  |2|, and expression levels at either time point that were 2 RPKM or greater.<sup>37–39</sup> Pathway analysis was performed on all genes whose expression was called “present” (>1 cpm in at least two samples) with DEGs defined as those exhibiting FC  $\geq$  |2| and FDR  $\leq$  0.05 using iPathwayGuide (Advaita Bioinformatics, Plymouth, MI, USA). This software package uses Impact Analysis, an approach that considers both whether DEGs participating in a particular pathway (as defined by the Kyoto Encyclopedia of Genes and Genomes, KEGG,<sup>40</sup> analysis performed with KEGG release 84.0+/-10-26, Oct 17) are overrepresented in the gene list and their directional interactions within the pathway.<sup>41</sup>

### Immunofluorescence

Immunofluorescence was performed to assay protein expression levels at the cellular level as described previously.<sup>42</sup> Briefly, eyes were embedded in Optimum Cutting Temperature Media (Tissue Tek, Torrance, CA, USA) immediately after harvest and stored at  $-80^{\circ}\text{C}$ . Frozen sections (16  $\mu\text{m}$ ) were obtained with a Leica CM3050 cryostat (Leica Microsystems, Buffalo Grove, IL, USA) and mounted on Color Frost plus slides (Fisher Scientific, Hampton, NH, USA). Sections were fixed in either 1:1 acetone-methanol for 15 minutes at  $-20^{\circ}\text{C}$  or 4% paraformaldehyde (PFA) for 15 minutes at room temperature (RT). After washing with PBS, slides were blocked for 1 hour at RT, then incubated with primary antibody diluted in blocking buffer (see Supplementary Table S1 for specifics on the primary antibodies, blocking buffer compositions, incubation times, and dilutions used in this study). Following primary antibody treatment, slides were washed three times with PBS, then incubated for 1 hour at RT with 1:200 dilution of species-appropriate Alexa Fluor 488- or 568-labeled secondary antibody (Invitrogen, Grand Island, NY, USA) in PBS. DNA/cell nuclei were detected by adding either a 1:2000 dilution of Draq5 (Biostatus Limited, Shepshed, Leicestershire, UK), or a 1:1000 dilution of 4',6-diamidino-2-phenylindole (DAPI; Fluoropure D21490; Thermo Fisher/Invitrogen, Carlsbad, CA, USA) to the secondary antibody solution. Some experiments also included a 1:250 dilution of fluorescein-labeled anti- $\alpha$ -SMA (Sigma-Aldrich Corp., St. Louis, MO, USA) in the secondary detection solution to visualize myofibroblasts. Slides were then washed with PBS three times and coverslipped using antifade mounting media. All slides were stored at  $-20^{\circ}\text{C}$  while awaiting analysis. Each staining experiment/time point was replicated using at least three independent specimens.

### Confocal Imaging

Fluorescently labeled slides were visualized using a Zeiss 780 LSM confocal microscope (Carl Zeiss, Inc., Gottingen, Germany), and comparisons between images were made



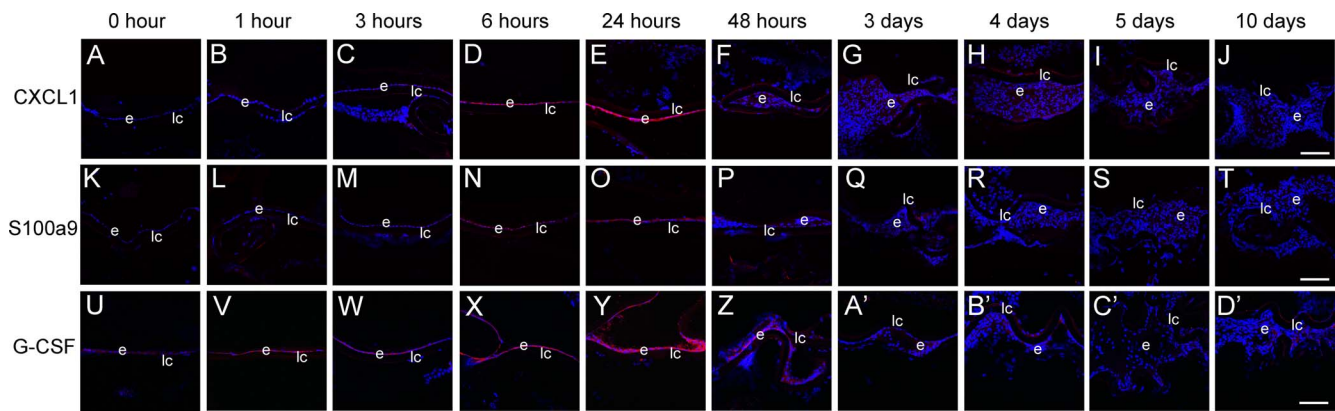


**FIGURE 2.** PCS expression time course in LECs for the three most differentially expressed genes in this study. (A–J) CXCL1 protein expression (*red*) in LECs after lens fiber removal. CXCL1 protein was not detected in LECs at 0 hour (A) and 1 hour (B) PCS. CXCL1 expression is first detected at 3 hours PCS (C), and this becomes robust by 6 hours PCS (D). The highest CXCL1 expression was detected at 24 hours PCS (E) followed by dramatic downregulation by 48 hours PCS (F). Weak CXCL1 expression persisted at 3 days PCS (G) and 4 days PCS (H), while almost no CXCL1 staining was detected at 5 days PCS (I) and 10 days PCS (J). (K–T) S100a9 protein expression (*red*) in LECs PCS. There is little to no S100a9 expression in LECs at 0 hour (K), 1 hour (L), and 3 hours (M) PCS. S100a9 protein levels upregulated by 6 hours PCS (N), peaked around 24 hours PCS (O), then downregulated by 48 hours PCS (P). Low-level S100a9 expression is associated with capsular bags during 3 days (Q), 4 days (R), and 5 days (S) PCS, but largely disappears by 10 days PCS (T). (U–D') G-CSF protein expression (*red*) in LECs PCS. Weak G-CSF staining was observed in LECs at 0 hour PCS (U), and this staining upregulated gradually between 1 hour (V), 3 hours (W), and 6 hours (X) PCS. The highest level of G-CSF staining was seen at 24 hours PCS (Y), while this was attenuated at 48 hours PCS (Z). G-CSF levels are nearly undetectable at 3 days (A'), 4 days (B'), 5 days (C'), and 10 days (D') PCS. For all parts of figure, *blue* indicates DNA as visualized by Draq5 staining; *scale bars*: 100  $\mu$ m; e, remnant lens epithelial cells/lens cells; lc, lens capsule.

response to cytokine (270 of 590 genes associated with the term; FDR corrected  $P = 1 \times 10^{-2}$ ), cytokine production (226 of 498 genes associated with the term; FDR corrected  $P = 3.5 \times 10^{-20}$ ), and the innate immune response (186 of 447 genes associated with the term; FDR corrected  $P = 3.7 \times 10^{-12}$ ).

### Lens Epithelial Cells Upregulate Diverse Genes Involved in the Inflammatory Response Within the First 24 Hours of Cataract Surgery

While cataract surgery is very effective, its short-term outcome is hampered by the onset of ocular inflammation by 24 hours PCS,<sup>58</sup> which is usually attributed to surgically induced breaks in the blood-aqueous barrier that allow for plasma protein leakage into the aqueous humor and immune cell infiltration. Since RNA-seq analysis revealed that the three genes most upregulated in LECs at 24 hours PCS were the mediators of innate immunity, *CXCL1* (3866-fold), *S100a9* (1505-fold), and *CSF3/G-CSF* (1119-fold) (Supplementary Table S2), we sought to determine their protein expression dynamics in lens capsular bags between 0 hour and 10 days PCS (Fig. 2). The expression of the chemokine *CXCL1*<sup>59</sup> was absent in capsular bags at 0 and 1 hour PCS (Figs. 2A, 2B) but was detected in LECs at 3 and 6 hours PCS (Figs. 2C, 2D). *CXCL1* protein levels peaked in LECs at 24 hours PCS (Fig. 2E), sharply downregulated in capsular bags by 48 hours PCS (Fig. 2F), and remained low between 3 and 10 days PCS (Figs. 2G–J).

The proinflammatory alarmin *S100a9*<sup>60</sup> was not detected in capsular bags isolated at 0 or 3 hours PCS (Figs. 2K–M). *S100a9* immunostaining was first detected in capsular bags at 6 hours PCS (Fig. 2N), which became more intense at 24 hours PCS (Fig. 2O). *S100a9* levels sharply downregulated in capsular bags by 48 hours PCS (Fig. 2P) and remained low between 3 and 10 days PCS (Figs. 2Q–T).

There was a weak immunolocalization signal for *CSF3* (granulocyte colony-stimulating factor, G-CSF, an important cytokine in neutrophil development<sup>61</sup>) in LECs immediately PCS (Fig. 2U). This staining became more intense at 1 hour PCS (Fig. 2V) and continued to increase through 6 hours PCS (Figs.

2W, 2X), peaking at 24 hours PCS (Fig. 2Y). G-CSF protein levels declined by 48 hours PCS (Fig. 2Z) and were nearly undetectable between 3 and 10 days PCS (Figs. 2A'–D').

In addition to the three most upregulated genes studied above, the RNA-seq data revealed that a number of other genes that function in diverse proinflammatory pathways were also upregulated in capsular bags at 24 hours PCS. *PTSG2*, the gene encoding the enzyme cyclooxygenase 2 (COX-2), which catalyzes a key step in prostaglandin synthesis,<sup>62</sup> was 248-fold upregulated in capsular bags at 24 hours PCS. COX-2 protein was not detected in capsular bags immediately PCS (Fig. 3A); however, weak COX-2 immunostaining was detected 1 hour PCS (Fig. 3B) and continued to increase through 6 hours (Figs. 3C, 3D) PCS, peaking at 24 hours PCS (Fig. 3E). COX-2 levels decline by 48 hours PCS (Fig. 3F), and remain low, but are detectable at 3 and 4 days PCS (Figs. 3G, 3H). However, significant COX-2 immunostaining was associated with capsular bags at 5 days PCS (Fig. 3I), although these levels again decreased by 10 days PCS (Fig. 3J).

*CCL2* encodes the chemokine, monocyte chemoattractant protein-1 (MCP-1),<sup>63</sup> whose mRNA levels are 92-fold upregulated in lens capsular bags at 24 hours PCS. No *CCL2* immunolabeling was detected in lens capsular bags either immediately or 3 to 6 hours PCS (Figs. 3K–M). Modest *CCL2* immunolocalization was detected in capsular bags from 6 to 48 hours PCS (Figs. 3N–P) but its levels decreased thereafter. *CCL2* protein was not detectable in capsular bags from 3 to 10 days PCS (Figs. 3Q–T).

*LCN2* (neutrophil gelatinase-associated lipocalin/lipocalin2) is a multifunctional protein often upregulated in stressed tissues, particularly following injury. It has antimicrobial activity via its ability to scavenge microbial-derived siderophores<sup>64</sup>; it binds to and stabilizes MMP9,<sup>64</sup> which is implicated in TGF $\beta$ -mediated LEC EMT,<sup>65</sup> while also inducing the synthesis of proinflammatory cytokines by neutrophils.<sup>64</sup> *LCN2* mRNA levels upregulate 60-fold in LECs by 24 hours PCS. *LCN2* protein was not detected in capsular bags at the time of surgery (Fig. 3U) but was found at modest levels at 1 and 3 hours PCS (Figs. 3V, 3W). *LCN2* levels further increase in

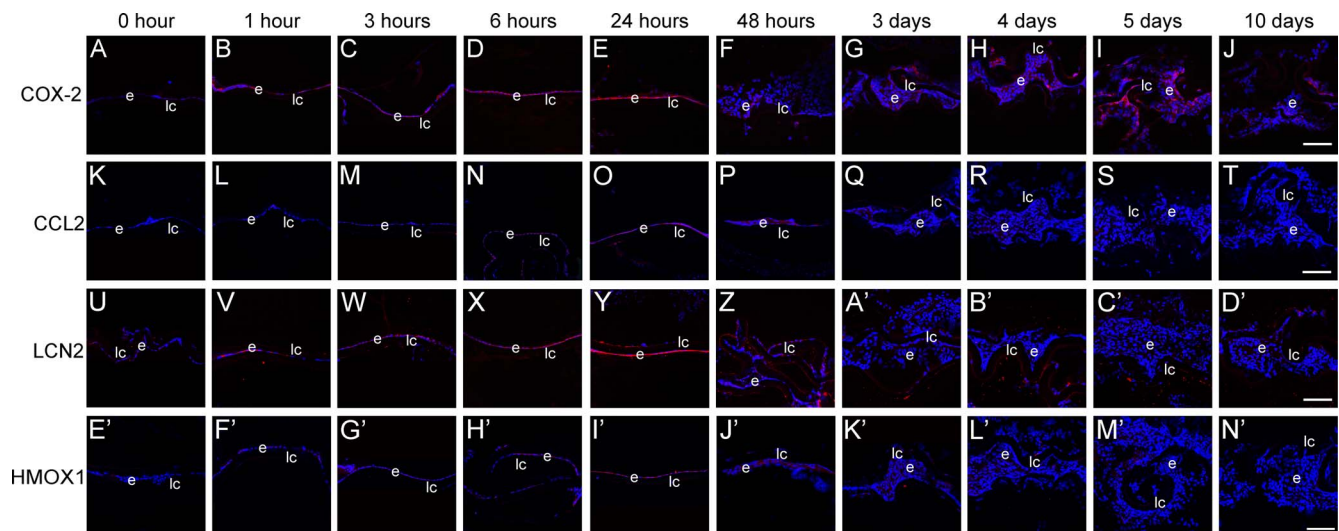


**FIGURE 3.** PCS expression time course for representative members of four different important inflammatory pathways in LECs. (A–J) COX-2 protein expression (*red*) in LECs PCS. COX-2 protein was not detected in LECs at 0 hour PCS (A), but it upregulated gradually between 1 hour (B), 3 hours (C), and 6 hours (D) PCS with peak at 24 hours PCS (E). COX-2 decreases by 48 hours (F), remains low at 3 days PCS (G), but is upregulated at 4 days (H) and 5 days (I) PCS. COX-2 levels are again low by 10 days (J) PCS. (K–T) CCL2 protein expression (*red*) in LECs after cataract surgery. Low COX-2 expression is observed in LECs at 0 hour (K), 1 hour (L), and 3 hours (M) PCS. CCL2 expression begins to upregulate by 6 hours (N) PCS, reaching a peak by 24 hours PCS (O) followed by a moderate decrease by 48 hours (P) PCS. By 3 days PCS (Q), CCL2 levels downregulate sharply and remain low through 4 days (R), 5 days (S), and 10 days (T) PCS. (U–D′) LCN2 protein expression (*red*) in LECs after cataract surgery. Minimal LCN2 expression was observed in LECs at 0 hour PCS (U), while it upregulated gradually between 1 hour (V), 3 hours (W), and 6 hours (X) PCS. After peaking at 24 hours PCS (Y), it is downregulated moderately by 48 hours PCS (Z) while it was essentially undetectable by 3 days PCS (A′). LCN2 levels remained low through 4 days (B′), 5 days (C′) and 10 days (D′) PCS. (E′–N′) HMOX1 protein expression (*red*) in LECs PCS. HMOX1 immunostaining was not detected in LECs at 0 hour (E′), 1 hour (F′) and 3 hours (G′) PCS. HMOX1 is first detected at 6 hours PCS (H′) and staining peaks at 24 hours PCS (I′). HMOX1 levels are decreased at 48 hours PCS (J′) while HMOX1 expression is not detected at 3 days (K′), 4 days (L′), 5 days (M′) and 10 days (N′) PCS. For all parts of figure, *blue* indicates DNA as visualized by DraQ5 staining; *scale bars*: 100 μm; e, remnant lens epithelial cells/lens cells; lc, lens capsule.

capsular bags at 6 hours PCS (Fig. 4X), and are maximal at 24 hours PCS (Fig. 3Y). LCN2 levels fall sharply by 48 hours PCS (Fig. 3Z, and are essentially undetectable between 3 and 10 days PCS (Figs. 3A′–D′).

Heme oxygenase (HMOX1) is an enzyme that catalyzes the degradation of hemoglobin into bilirubin and carbon monoxide, which modulates innate and adaptive immunity while protecting cells from inflammation-induced oxidative stress.<sup>66</sup> RNA-seq revealed that *HMOX1* mRNA levels are 27-fold upregulated in lens capsular bags at 24 hours PCS compared to 0 hour PCS. No HMOX1 protein was detectable by immunolocalization in lens capsular bags between the time of surgery and 3 hours PCS (Figs. 3E′–G′). Modest HMOX1 staining was detected in lens capsular bags between 6 and 48 hours PCS (Figs. 3H′–J′), while HMOX1 staining was absent from capsular bags between 3 and 10 days PCS (Figs. 3K′–N′).

These data in aggregate reveal that LECs rapidly initiate an inflammatory response after cataract surgery and/or lens wounding.

### Inflammatory Cells Are Associated With the Lens Capsular Bag Post Cataract Surgery

As many of the genes induced in lens capsular bags at 24 hours PCS are known chemokines that can attract neutrophils to injury sites, we then determined the timing of leukocyte infiltration into the mouse eye PCS. Immunostaining of lens capsular bags PCS with CD11b (*ITGAM*, integrin alphaM, 9-fold upregulated in lens capsular bags at 24 hours PCS by RNA-seq), a widely accepted cell surface leukocyte marker with known roles in inflammation,<sup>67</sup> revealed no leukocyte infiltration into the eye prior to 12 hours PCS (Figs. 4A–C, 4K–M), while the

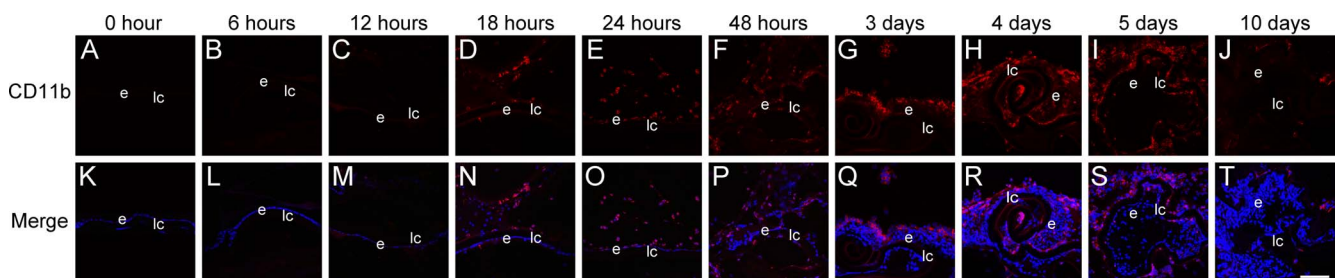


**FIGURE 4.** Neutrophil infiltration into the lens capsular bag PCS identified by CD11b immunostaining. (A–J) CD11b (*red*) staining alone; (K–T) CD11b expression (*red*) is merged with DNA detected by DraQ5 (*blue*). No CD11b-positive neutrophils are seen at 0 hour (A, K), 6 hours (B, L), and 12 hours (C, M) PCS. The first CD11b-positive neutrophils are observed at 18 hours PCS (D, N), then increase by 24 hours PCS (E, O) and remain abundant through 48 hours (F, P), 3 days PCS (G, Q), 4 days PCS (H, R), and 5 days PCS (I, S). However, the number of CD11b-positive cells sharply decreases by 10 days PCS (J, T). *Scale bars*: 100 μm. e, remnant lens epithelial cells/lens cells; lc, lens capsule.

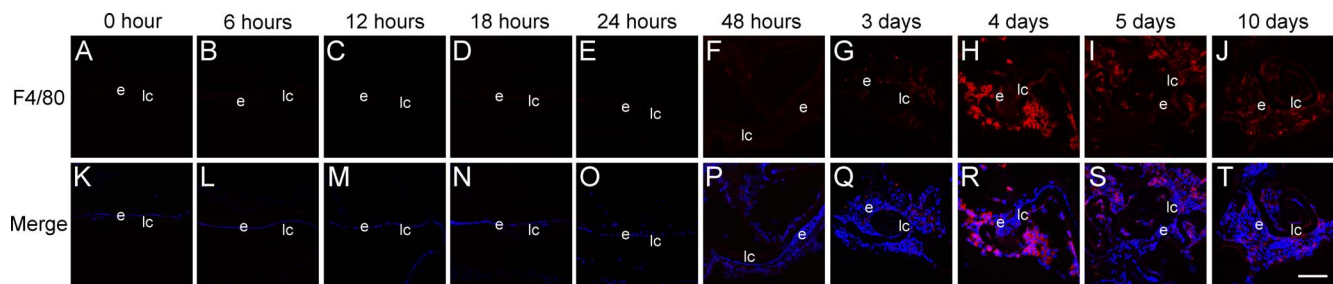


**FIGURE 5.** Macrophage infiltration into lens capsular bags following cataract surgery identified by F4/80 immunostaining. (A–J) F4/80 expression alone (*red*). (K–T) Merge between F4/80 immunodetection (*red*) and nuclear staining as detected by Draq5 labeling of DNA (*blue*). No F4/80 staining (*red*) is seen at 0 hour (A, K), 6 hours (B, L), 12 hours (C, M), 18 hours (D, N), and 24 hours (E, O) PCS. The first F4/80-positive cells are detected at 48 hours PCS (F, P) and robust numbers of F4/80-positive cells are first seen at 3 days PCS (G, Q), and increase dramatically at 4 days PCS (H, R). Robust numbers of F4/80-positive cells are maintained at 5 days (I, S) and 10 days (J, T) PCS. Scale bars: 100  $\mu$ m; e, remnant lens epithelial cells/lens cells; lc, lens capsule.

first CD11b-positive cells associated with lens capsular bags were detected at 18 hours PCS (Figs. 4D, 4N). The abundance of CD11b-positive cells increases from 18 hours to 3 days PCS, remains appreciable at 4 and 5 days PCS, then falls to low levels by 10 days PCS. Similar results were obtained by immunostaining capsular bags with LY-6G, a GPI-linked protein that is a recognized marker of granulocytes and peripheral neutrophils.<sup>68</sup> Similar to CD11b, the first LY-6G-positive cells did not arrive in the lens capsular bag until 18 hours PCS, although fewer cells stained overall (Supplementary Fig. S2) as would be expected since LY-6G is found on a more restricted set of leukocytes.

Since CD11b immunostaining is unable to distinguish between neutrophils and macrophages, we then immunostained capsular bags PCS with F4/80, an antibody that detects *EMRI*, a glycoprotein that is a very abundant and specific marker for mouse macrophages.<sup>69</sup> This experiment revealed that no F4/80-positive macrophages are associated with lens capsular bags for the first 24 hours PCS (Figs. 5A–E, 5K–O) as expected since the *EMRI* gene is not appreciably expressed in capsular bags right after surgery, and is not differentially expressed in 24-hour PCS capsular bags by RNA-seq (not shown). While occasional F4/80-positive cells were detected at 48 hours PCS (Figs. 5F, 5P; not shown), the first appreciable numbers of F4/80-positive cells were associated with lens capsular bags at 3 days PCS (Figs. 5G, 5Q), while they become more abundant at 4 and 5 days PCS (Figs. 5H, 5I, 5R, 5S). F4/80-positive cells are still associated with lens capsular bags at 10 days PCS (Fig. 5J, 5T).

### Proinflammatory Cytokines Colocalize With the Epithelial Marker, $\beta$ 1-Integrin, in Lens Epithelial Cells at 24 Hours PCS, and in $\alpha$ -SMA-Positive Lens Cells at 48 Hours PCS, While These Molecules Generally Were Not Found at High Levels in Infiltrating Leukocytes

As most of the cytokines tested have been reported to be expressed by leukocytes, we then performed colocalization studies to confirm whether these genes were activating in LECs PCS, or whether the upregulation of these genes was simply reflecting leukocyte infiltration into the eye. Thus, we colocalized the cytokines of interest with  $\beta$ 1-integrin, which is known to be abundant in LECs, particularly PCS,<sup>33</sup> where it plays key roles in regulating the communication of lens cells with the capsule.<sup>70,71</sup> This analysis revealed that all seven immune regulators studied, CXCL1, S100a9, G-CSF, COX-2, CCL2, LCN2, and HMOX1, showed a near-complete overlap

with  $\beta$ 1-integrin-positive LECs at 24 hours PCS (Supplementary Fig. S3). Further, double immunolabelling of 24 hours PCS lens capsular bags for the cytokines of interest and the leukocyte marker CD11b revealed that CXCL1, G-CSF, COX-2, CCL2, and LCN2 did not colocalize with CD11b-positive cells (Supplementary Fig. S4). In contrast, the alarmin S100a9 was found in both LECs and a subset of CD11b-positive cells (Supplementary Fig. S4), which would be expected as S100a9 has been reported to make up 40% of the cytoplasmic protein of circulating neutrophils.<sup>72</sup>

In this cataract surgery model, the first induction of the fibrotic marker  $\alpha$ -SMA protein is seen in remnant LECs at 48 hours PCS.<sup>33</sup> Coimmunostaining of the tested cytokines (purple) with CD11b (red) and  $\alpha$ -SMA (green) revealed that these proinflammatory markers were generally expressed in  $\alpha$ -SMA-positive lens cells, not CD11b-positive leukocytes at this stage (Fig. 6). The exception was S100a9, which was observed in both  $\alpha$ -SMA-positive lens cells as well as CD11b-positive leukocytes (Fig. 6, arrows).

While six of the seven inflammatory modulators showed a peak of expression in LECs at 24 hours PCS, followed by a rapid downregulation, COX-2 showed a biphasic response, with the first upregulation seen at 24 hours followed by a rapid fall at 48 hours PCS (Figs. 3A–G, 7A–C), while the second increase started at 4 days PCS with a peak in COX-2 levels in 5 days PCS capsular bags (Figs. 3H–J, 7D–F). As this second wave of COX-2 immunostaining matches the timing of macrophage infiltration into capsular bags (Figs. 5G–J), and COX-2 has been reported to be abundant in macrophages,<sup>73</sup> we performed coimmunostaining of F4/80 (red) with COX-2 (green) (Fig. 7). As expected, the second wave of COX-2 expression corresponds with the influx of F4/80-positive macrophages at 4 days PCS; however, while some overlap between COX-2- and F4/80-positive cells is seen, the majority of COX-2 staining in capsular bags between 4 and 10 days PCS did not colocalize with F4/80 (Fig. 7).

### Macrophage Influx and Upregulation of SMAD3 Phosphorylation (pSMAD3) During Fibrosis Post Cataract Surgery

Canonical (i.e., SMAD mediated) TGF $\beta$  signaling is recognized to be a major mediator of fibrotic PCO.<sup>74</sup> However, TGF- $\beta$  is produced in an inactive form and must be activated by tightly controlled mechanisms to elicit signaling.<sup>75</sup> As macrophages have been implicated in the activation of TGF $\beta$  driving some fibrotic diseases,<sup>76,77</sup> we compared the timing of macrophage influx into the lens capsular bag PCS with the onset of robust

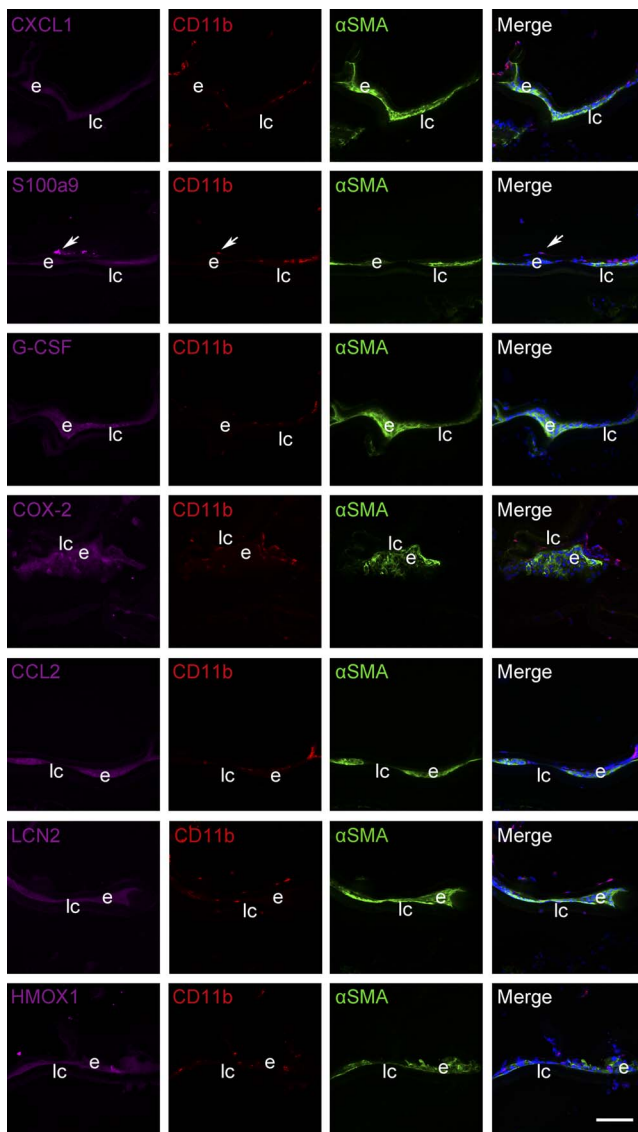


**FIGURE 6.** The residual proinflammatory gene expression detected in lens capsular bag-associated cells at 48 hours PCS colocalizes with the fibrotic marker,  $\alpha$ -SMA. Triple immunostaining of inflammatory cytokines (purple) with CD11b (red) and  $\alpha$ -SMA (green) in capsular bags isolated at 48 hours PCS. Most inflammatory cytokine-positive cells (purple) colocalized with  $\alpha$ -SMA (green), but not CD11b-positive cells (red), although some CD11b-positive cells were also S100a9 positive (arrows). Merge: cytokine (purple), CD11b (red),  $\alpha$ -SMA (green); nuclei stained with the DNA dye DAPI (blue). Scale bars: 100  $\mu$ m. e, remnant lens epithelial cells/lens cells; lc, lens capsule.

SMAD3 phosphorylation in remnant lens cells PCS (Fig. 8). As we previously reported,<sup>33</sup> pSMAD3 is undetectable by immunostaining in lens capsular bags prior to 24 hours PCS, while the first pSMAD3-positive nuclei are first detected in capsular bags at 48 hours PCS, although the staining is relatively weak (Figs. 7, 8). A robust upregulation of pSMAD3 staining in lens cells occurs between 48 hours and 3 days PCS, which corresponds to initial major influx of F4/80-positive macrophages into the area surrounding the capsular bag. The levels of pSMAD3 remain easily detectable in lens cells from 4 to 10 days PCS, and these cells are in close proximity to F4/80-positive macrophages (Fig. 8).

## DISCUSSION

The EMT of LECs to myofibroblasts is recognized to produce the fibrotic tissue seen in ASC as well as the fibrotic sequelae of cataract surgery including Soemmering's ring and the various forms of visual axis opacification (VAO) including anterior capsular contraction/phimosis, PCO, and VAO due to growth of myofibroblasts along the anterior hyaloid membrane.<sup>43,74</sup> There is robust experimental evidence supporting the hypothesis that canonical TGF $\beta$  signaling is both sufficient and necessary to induce LEC EMT,<sup>22,24,78</sup> while the main signal transducer of the canonical TGF $\beta$  pathway (pSMAD2/3) is detected in both ASCs<sup>25,79</sup> and fibrotic lens capsular bags, even years after surgery.<sup>25</sup> However, TGF $\beta$  is produced in a latent form and must be activated to elicit signaling,<sup>30,80</sup> and we have previously shown that there is a 48-hour lag between lens injury and the ability to detect pSMAD2/3 in LECs in a mouse cataract surgery model.<sup>33</sup> This work sought to elucidate the early response of LECs to cataract surgery that sets up the conditions necessary for the onset of TGF $\beta$  signaling and LEC EMT.

### Lens Epithelial Cells Rapidly Change Their Phenotype in Response to Surgical Lens Fiber Cell Removal

LECs are polarized epithelial cells with basal attachments on the lens capsule and apical interactions with the apical tips of lens fiber cells.<sup>81</sup> These cells normally express many of the classical markers of an epithelium while also expressing genes more specific for lens function.<sup>82</sup> Comparison of the LEC transcriptome at the time of surgery with LECs remaining in the eye for 24 hours PCS revealed that many genes known to be important for the lens phenotype exhibit altered expression. As expected for an EMT response, many regulators of lens cell fate and structure are downregulated, including *Sipa1l3*,<sup>44</sup> *Foxe3*,<sup>47</sup> *Tdrd7*,<sup>50</sup> *Maf*,<sup>51</sup> *Pitx3*,<sup>51</sup> *Hsf4*,<sup>51</sup> *FoxE3*,<sup>83</sup> and *Pax6*.<sup>53</sup> However, at least five genes known to be important for lens development or physiology are upregulated PCS, including *Vim*,<sup>52</sup> *Wfs1*,<sup>54</sup> *Epba2*,<sup>55</sup> *Fll1*,<sup>56</sup> and *Gcnt2*.<sup>57</sup> It is notable though that some of these upregulated genes are regulators or markers of mesenchymal cell fate or fibrosis<sup>84-86</sup> in other systems, suggesting that their increased expression PCS also reflects the onset of LEC EMT. Finally, we detect the upregulation of transcripts encoding many myofibroblast markers in LECs at 24 hours PCS including  $\alpha$ -SMA, tenascin C, TGF $\beta$ i, fibronectin, transgelin, lysyl oxidase, collagen type I, and  $\alpha$ 5-integrin. As we are unable to detect the pSMAD2/3 indicative of TGF $\beta$  signaling in LECs at this time point (Fig. 8), this implies that the initial fibrotic response of LECs PCS is independent of TGF $\beta$  signaling, although it is possible that some TGF $\beta$  signaling is active but is below the threshold of our pSMAD2/3 detection assay.

### Lens Epithelial Cells Remaining Behind PCS Rapidly Induce the Expression of Genes Important for the Innate Immune Response

The uninjured lens epithelium expresses few genes with known roles in the innate immune response. However, RNA-seq coupled with immunofluorescence revealed that a large number of genes involved in innate immunity, including those involved in numerous cytokine pathways, the prostaglandin synthesis pathway, and interleukins, were highly induced in LECs by 24 hours PCS. Many of the most upregulated genes encode either chemoattractants that induce neutrophil/macrophage/monocyte migration from the circulation to injury sites

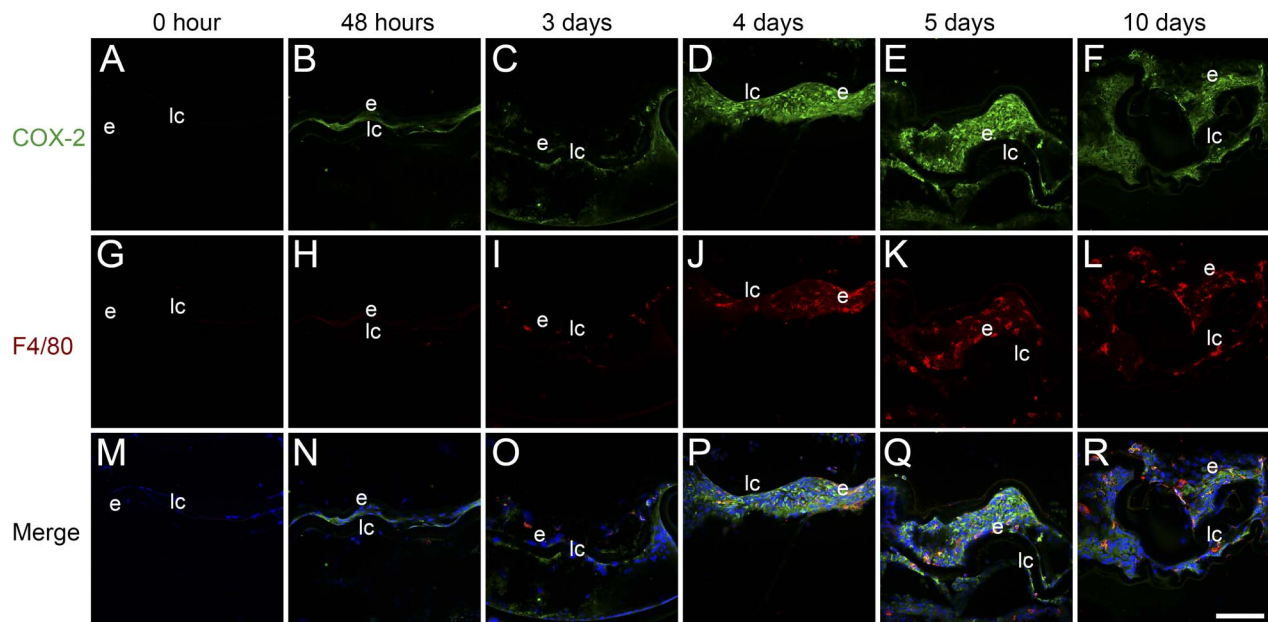


**FIGURE 7.** The late upregulation of COX-2 protein levels PCS observed in lens capsular bags only partially colocalizes with F4/80-positive macrophages. (A–F) COX-2 protein localization (*green*) alone. (G–L) F4-80 expression alone (*red*). (M–R) Merge between F4-80 immunodetection (*red*), COX-2 immunostaining (*green*), and nuclear staining as detected by Draq5 labeling of DNA (*blue*). No F4/80 or COX-2 immunostaining is seen at 0 hours (A, G, M). At 48 hours PCS, only the occasional F4-80-positive cell is detected and these do not stain strongly for COX-2 (B, H, N). At 3 days PCS, COX-2 levels are low in all cells associated with capsular bags, although F4/80-positive cell numbers are increasing (C, I, O). At 4 days PCS, COX-2 levels increase in most capsular bag cells and some colocalization of COX-2 staining in F4/80-positive cells is seen (D, J, P), a pattern that is similar at 5 days PCS (E, K, Q). By 10 days PCS, the numbers of F4/80-positive cells appear to decline along with the intensity of COX-2 immunostaining (F, L, R). *Scale bars:* 100  $\mu\text{m}$ . e, remnant lens epithelial cells/lens cells; lc, lens capsule.

or modulate innate immune responses as would be expected after wounding of any epithelium.

Notably, though, it appears that the details of the initial inflammatory cascade initiated by LECs may be unique to the lens. While RNA-seq experiments testing the early stages of abrasive wound healing in mouse skin are qualitatively consistent with our results in lens as mRNAs for genes involved in the cytokine response are elevated by 12 hours post wounding, remain quite high at 24 hours post wounding, and generally fall by 36 hours post wounding, none of the six genes that we highlighted for study in LECs (the top three most upregulated plus three others of biological interest) were included in the top 100 changed genes in abrasive skin wounding in mice.<sup>87</sup> Further, the responses appear quite different quantitatively as well. For instance, while *CXCL1* (the most elevated gene in LECs PCS) is also elevated after abrasive skin wounding, the response is much more muted than in LECs while COX-2, whose mRNA is elevated 248-fold in LECs PCS, is not altered in skin post abrasive wounding at any time tested.<sup>87</sup> The diversity of transcriptional responses to wounding is further highlighted by a recent paper demonstrating that human oral mucosa and skin have very different responses to incisional wounding, largely because the naïve oral mucosa already expresses many genes usually associated with inflammation, including *S100A8/A9* (which are among the top upregulated genes in injured lens epithelium, while *CXCL1* and *CCL2* (other top upregulated genes in injured mouse lens epithelium) do not upregulate after mucosal injury but are upregulated 48 hours and 5 days after incisional wounding of human skin.<sup>88</sup>

Notably, human LECs have been previously reported to synthesize interleukins, prostaglandins, and G-CSF in culture,<sup>89,90</sup> while the time course of inflammatory cell arrival in

the mouse eye PCS is similar to the timing of the onset of “flare plus cells” in humans PCS.<sup>91</sup> This suggests that the mouse cataract surgery model used in this study may accurately reflect the ocular inflammatory response subsequent to human cataract surgery. However, this requires confirmation as different species can induce different inflammatory responses to the same insult.<sup>92,93</sup> Further, as most human cataract surgeries are performed on people who are elderly while the results presented here were obtained on young adult mice, it will be important to test how age affects the postsurgical inflammatory response in the mouse model, as it has been previously reported that LECs from elderly people produce a different profile of interleukins than those from younger individuals when cultured under serum-free conditions in an *in vitro* organ culture PCO model.<sup>90</sup> Finally, little is known about the inflammatory cell types infiltrating the human eye PCS, and neither the timing nor the identity of the major cytokines upregulated by human LECs PCS is known.

### Possible Significance of Postsurgical Inflammation

We found that the upregulation of the innate immune response in LECs likely occurs rapidly PCS as the levels for all of the proinflammatory proteins tested were elevated by 6 hours PCS, preceding the arrival of neutrophils into the eye PCS by at least 12 hours, and the arrival of macrophages by 2 to 3 days. Notably, we find that inflammatory mediators upregulate at least a day prior to TGF $\beta$  signaling PCS, while it is known that eyes with active inflammation (such as in uveitis) are more prone to aggressive fibrosis PCS.<sup>94,95</sup> Thus, it is possible that the inflammatory response seen in LECs post wounding is an initiator of PCO. Several prior studies have attempted to



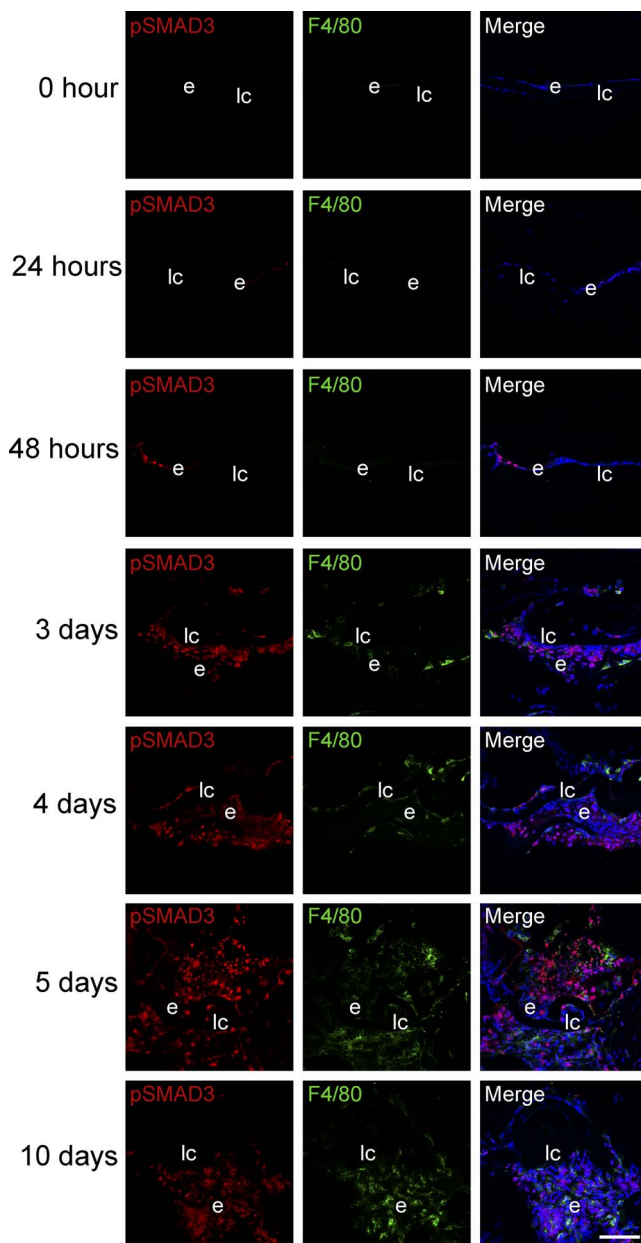


**FIGURE 8.** Upregulation of pSMAD3 in LECs PCS correlates with the timing of F4/80-positive macrophage infiltration into lens capsular bags PCS. Neither pSMAD3 staining (red) nor F4/80-positive cells (green) are detected in lens capsular bags analyzed either immediately PCS or 24 hours later. The first pSMAD3 nuclei (red) are detected at 48 hours PCS, while both staining intensity and number of pSMAD3-positive nuclei gradually increase through 3 and 4 days PCS, peaking at 5 days PCS. Occasional F4/80-positive macrophages (see Fig. 6) are detected at 48 hours PCS, but their numbers increase sharply by 3 days PCS, and these cells remain abundant in the capsular bag through 10 days PCS. Merge: pSMAD3 (red); F4/80 (green); nuclei stained with the DNA dye Draq5 (blue). Scale bars: 100  $\mu$ m. e, remnant lens epithelial cells/lens cells; lc, lens capsule.

determine whether aggressive prevention of postsurgical inflammation can ameliorate PCO; however, the results are equivocal.<sup>27,34,96-99</sup> However, in each case, only a subset of the proinflammatory pathways active PCS have been targeted, so these studies do not definitively rule out the therapeutic potential of shutting down PCS inflammation in PCO prevention.

## CONCLUSIONS

The past several decades have seen numerous advances in cataract surgery techniques and IOL implants, which have yielded huge decreases in the number of people suffering from blindness or visual disability due to cataract.<sup>1,4</sup> Despite these advances, postsurgical inflammation and ocular fibrosis derived from EMT of residual LECs are still significant barriers preventing ideal visual outcomes.<sup>9,100-102</sup> Overall, this study provides new insights into the pathophysiology of cataract surgery side effects and implies that the LECs remaining behind following cataract surgery are signaling centers promoting PCS inflammation.

## Acknowledgments

The authors thank Samuel Novo for critical reading of the manuscript.

Supported by National Eye Institute Grants EY015279 and EY028597 to MKD. Xiaobo Xia, MD, Chair, Ophthalmology, Xiangya Hospital, supported JJ's sabbatical leave in the Duncan lab, and The Delaware INBRE program, supported by a grant from the National Institute of General Medical Science (NIGMS; P20 GM103446) and the State of Delaware, supported the RNA-seq analysis and the University of Delaware Bioimaging Facility. The authors alone are responsible for the content and writing of the paper.

Disclosure: **J. Jiang**, None; **M.H. Shihan**, None; **Y. Wang**, None; **M.K. Duncan**, None

## References

- Olson RJ. Cataract surgery from 1918 to the present and future—just imagine! *Am J Ophthalmol.* 2018;185:10-13.
- Liu YC, Wilkins M, Kim T, Malyugin B, Mehta JS. Cataracts. *Lancet.* 2017;390:600-612.
- Khairallah M, Kahloun R, Bourne R, et al. Number of people blind or visually impaired by cataract worldwide and in world regions, 1990 to 2010. *Invest Ophthalmol Vis Sci.* 2015;56:6762-6769.
- Lee CM, Afshari NA. The global state of cataract blindness. *Curr Opin Ophthalmol.* 2017;28:98-103.
- Wormstone IM, Wang L, Liu CS. Posterior capsule opacification. *Exp Eye Res.* 2009;88:257-269.
- Bhattacharjee H, Deshmukh S. Soemmering's ring. *Indian J Ophthalmol.* 2017;65:1489.
- Spalton DJ, Russell SL, Evans-Gowing R, Eldred JA, Wormstone IM. Effect of total lens epithelial cell destruction on intraocular lens fixation in the human capsular bag. *J Cataract Refract Surg.* 2014;40:306-312.
- Alio JL, Ben-nun J, Rodriguez-Prats JL, Plaza AB. Visual and accommodative outcomes 1 year after implantation of an accommodating intraocular lens based on a new concept. *J Cataract Refract Surg.* 2009;35:1671-1678.
- Spalton D. Preventing PCO. In: *ASCRS: EyeWorld*; February 2011. Available at: <https://www.eyeworld.org/article-preventing-pco>.
- Gimbel HV, Venkataraman A. Secondary in-the-bag intraocular lens implantation following removal of Soemmering ring contents. *J Cataract Refract Surg.* 2008;34:1246-1249.
- Michael K, O'Colmain U, Vallance JH, Cormack TG. Capsule contraction syndrome with haptic deformation and flexion. *J Cataract Refract Surg.* 2010;36:686-689.
- Epstein RH, Liu ET, Werner L, Kohnen T, Kaproth OK, Mamalis N. Capsulorhexis phimosis with anterior flexing of an accommodating IOL: case report and histopathological analyses. *J Cataract Refract Surg.* 2014;40:148-152.

13. Awasthi N, Guo S, Wagner BJ. Posterior capsular opacification: a problem reduced but not yet eradicated. *Arch Ophthalmol*. 2009;127:555-562.
14. Apple DJ, Escobar-Gomez M, Zaugg B, Kleinmann G, Borkenstein AF. Modern cataract surgery: unfinished business and unanswered questions. *Surv Ophthalmol*. 2011;56:S3-S53.
15. Khaja WA, Verma M, Shoss BL, Yen KG. Visual axis opacification in children. *Ophthalmology*. 2011;118:224-225.
16. Elkin ZP, Piluek WJ, Fredrick DR. Revisiting secondary capsulotomy for posterior capsule management in pediatric cataract surgery. *J AAPOS*. 2016;20:506-510.
17. Ronbeck M, Kugelberg M. Posterior capsule opacification with 3 intraocular lenses: 12-year prospective study. *J Cataract Refract Surg*. 2014;40:70-76.
18. Chan E, Mahroo OA, Spalton DJ. Complications of cataract surgery. *Clin Exp Optom*. 2010;93:379-389.
19. Billotte C, Berdeaux G. Adverse clinical consequences of neodymium:YAG laser treatment of posterior capsule opacification. *J Cataract Refract Surg*. 2004;30:2064-2071.
20. Burq MA, Taqui AM. Frequency of retinal detachment and other complications after neodymium:Yag laser capsulotomy. *J Pak Med Assoc*. 2008;58:550-552.
21. Wesolosky JD, Tennant M, Rudnisky CJ. Rate of retinal tear and detachment after neodymium:YAG capsulotomy. *J Cataract Refract Surg*. 2017;43:923-928.
22. de Iongh RU, Wederell E, Lovicu FJ, McAvoy JW. Transforming growth factor-beta-induced epithelial-mesenchymal transition in the lens: a model for cataract formation. *Cells Tissues Organs*. 2005;179:43-55.
23. Saika S, Miyamoto T, Ishida I, et al. TGFbeta-Smad signalling in postoperative human lens epithelial cells. *Br J Ophthalmol*. 2002;86:1428-1433.
24. Saika S, Kono-Saika S, Ohnishi Y, et al. Smad3 signaling is required for epithelial-mesenchymal transition of lens epithelium after injury. *Am J Pathol*. 2004;164:651-663.
25. Ishida I, Saika S, Okada Y, Ohnishi Y. Growth factor deposition in anterior subcapsular cataract. *J Cataract Refract Surg*. 2005;31:1219-1225.
26. Maier P, Broszinski A, Heizmann U, Boehringer D, Reinhard T. Determination of active TGF-beta2 in aqueous humor prior to and following cryopreservation. *Mol Vis*. 2006;12:1477-1482.
27. Nibourg LM, Gelens E, Kuijer R, Hooymans JM, van Kooten TG, Koopmans SA. Prevention of posterior capsular opacification. *Exp Eye Res*. 2015;136:100-115.
28. Srinivasan Y, Lovicu FJ, Overbeek PA. Lens-specific expression of transforming growth factor beta1 in transgenic mice causes anterior subcapsular cataracts. *J Clin Invest*. 1998;101:625-634.
29. Eldred JA, Dawes LJ, Wormstone IM. The lens as a model for fibrotic disease. *Philos Trans R Soc Lond B Biol Sci*. 2011;366:1301-1319.
30. Mamuya FA, Duncan MK.  $\alpha$ V integrins and TGF-beta-induced EMT: a circle of regulation. *J Cell Mol Med*. 2012;16:445-455.
31. Desai VD, Wang Y, Simirskii VN, Duncan MK. CD44 expression is developmentally regulated in the mouse lens and increases in the lens epithelium after injury. *Differentiation*. 2010;79:111-119.
32. Manthey AL, Terrell AM, Wang Y, Taube JR, Yallowitz AR, Duncan MK. The Zeb proteins  $\delta$ EF1 and Sip1 may have distinct functions in lens cells following cataract surgery. *Invest Ophthalmol Vis Sci*. 2014;55:5445-5455.
33. Mamuya FA, Wang Y, Roop VH, Scheiblin DA, Zajac JC, Duncan MK. The roles of  $\alpha$ V integrins in lens EMT and posterior capsular opacification. *J Cell Mol Med*. 2014;18:656-670.
34. Lewis AC. Interleukin-6 in the pathogenesis of posterior capsule opacification and the potential role for interleukin-6 inhibition in the future of cataract surgery. *Med Hypotheses*. 2013;80:466-474.
35. Kalari KR, Nair AA, Bhavsar JD, et al. MAP-RSeq: Mayo analysis pipeline for RNA sequencing. *BMC Bioinformatics*. 2014;15:224.
36. Robinson MD, McCarthy DJ, Smyth GK. edgeR: a bioconductor package for differential expression analysis of digital gene expression data. *Bioinformatics*. 2010;26:139-140.
37. Manthey AL, Lachke SA, FitzGerald PG, et al. Loss of Sip1 leads to migration defects and retention of ectodermal markers during lens development. *Mech Dev*. 2014;131:86-110.
38. Manthey AL, Terrell AM, Lachke SA, Polson SW, Duncan MK. Development of novel filtering criteria to analyze RNA-sequencing data obtained from the murine ocular lens during embryogenesis. *Genom Data*. 2014;2:369-374.
39. Audette DS, Anand D, So T, et al. Prox1 and fibroblast growth factor receptors form a novel regulatory loop controlling lens fiber differentiation and gene expression. *Development*. 2016;143:318-328.
40. Kanehisa M, Furumichi M, Tanabe M, Sato Y, Morishima K. KEGG: new perspectives on genomes, pathways, diseases and drugs. *Nucleic Acids Res*. 2017;45:D353-D361.
41. Tarca AL, Draghici S, Khatri P, et al. A novel signaling pathway impact analysis. *Bioinformatics*. 2009;25:75-82.
42. Reed NA, Oh D-J, Czymmek KJ, Duncan MK. An immunohistochemical method for the detection of proteins in the vertebrate lens. *J Immunol Methods*. 2001;253:243-252.
43. Shirai K, Tanaka SI, Lovicu FJ, Saika S. The murine lens: a model to investigate in vivo epithelial-mesenchymal transition. *Dev Dyn*. 2018;247:340-345.
44. Greenlees R, Mihelec M, Yousoof S, et al. Mutations in SIPA1L3 cause eye defects through disruption of cell polarity and cytoskeleton organization. *Hum Mol Genet*. 2015;24:5789-5804.
45. Santhiya ST, Kumar GS, Sudhakar P, et al. Molecular analysis of cataract families in India: new mutations in the CRYBB2 and GJA3 genes and rare polymorphisms. *Mol Vis*. 2010;16:1837-1847.
46. Chepelinsky AB. Structural function of MIP/aquaporin 0 in the eye lens; genetic defects lead to congenital inherited cataracts. *Handb Exp Pharmacol*. 2009;190:265-297.
47. Bremond-Gignac D, Bitoun P, Reis LM, Copin H, Murray JC, Semina EV. Identification of dominant FOXE3 and PAX6 mutations in patients with congenital cataract and aniridia. *Mol Vis*. 2010;16:1705-1711.
48. Gong X, Cheng C, Xia CH. Connexins in lens development and cataractogenesis. *J Membr Biol*. 2007;218:9-12.
49. Jakobs PM, Hess JE, FitzGerald PG, Kramer P, Weleber RG, Litt M. Autosomal-dominant congenital cataract associated with a deletion mutation in the human beaded filament protein gene BFSP2. *Am J Hum Genet*. 2000;66:1432-1436.
50. Lachke SA, Alkuraya FS, Kneeland SC, et al. Mutations in the RNA granule component TDRD7 cause cataract and glaucoma. *Science*. 2011;331:1571-1576.
51. Anand D, Agrawal SA, Slavotinek A, Lachke SA. Mutation update of transcription factor genes FOXE3, HSF4, MAF, and PITX3 causing cataracts and other developmental ocular defects. *Hum Mutat*. 2018;39:471-494.
52. Ma AS, Grigg JR, Ho G, et al. Sporadic and familial congenital cataracts: mutational spectrum and new diagnoses using next-generation sequencing. *Hum Mutat*. 2016;37:371-384.
53. Hingorani M, Williamson KA, Moore AT, van Heyningen V. Detailed ophthalmologic evaluation of 43 individuals with

- PAX6 mutations. *Invest Ophthalmol Vis Sci.* 2009;50:2581-2590.
54. Berry V, Gregory-Evans C, Emmett W, et al. Wolfram gene (WFS1) mutation causes autosomal dominant congenital nuclear cataract in humans. *Eur J Hum Genet.* 2013;21:1356-1360.
  55. Dave A, Martin S, Kumar R, Craig JE, Burdon KP, Sharma S. Epha2 mutations contribute to congenital cataract through diverse mechanisms. *Mol Vis.* 2016;22:18-30.
  56. Vanita V, Hejtmancik JF, Hennies HC, et al. Sutural cataract associated with a mutation in the ferritin light chain gene (FTL) in a family of Indian origin. *Mol Vis.* 2006;12:93-99.
  57. Irum B, Khan SY, Ali M, et al. Deletion at the GCNT2 locus causes autosomal recessive congenital cataracts. *PLoS One.* 2016;11:e0167562.
  58. El-Harazi SM, Feldman RM. Control of intra-ocular inflammation associated with cataract surgery. *Curr Opin Ophthalmol.* 2001;12:4-8.
  59. Kobayashi Y. The role of chemokines in neutrophil biology. *Front Biosci.* 2008;13:2400-2407.
  60. Austermann J, Zenker S, Roth J. S100-alarmins: potential therapeutic targets for arthritis. *Expert Opin Ther Targets.* 2017;21:739-751.
  61. Panopoulos AD, Watowich SS. Granulocyte colony-stimulating factor: molecular mechanisms of action during steady state and "emergency" hematopoiesis. *Cytokine.* 2008;42:277-288.
  62. Alexanian A, Miller B, Chesnik M, Mirza S, Sorokin A. Post-translational regulation of COX-2 activity by FYN in prostate cancer cells. *Oncotarget.* 2014;5:4232-4243.
  63. Yoshimura T. The chemokine MCP-1 (CCL2) in the host interaction with cancer: a foe or ally? *Cell Mol Immunol.* 2018;15:335-345.
  64. Moschen AR, Adolph TE, Gerner RR, Wieser V, Tilg H. Lipocalin-2: a master mediator of intestinal and metabolic inflammation. *Trends Endocrinol Metab.* 2017;28:388-397.
  65. Korol A, Pino G, Dwivedi D, Robertson JV, Deschamps PA, West-Mays JA. Matrix metalloproteinase-9-null mice are resistant to TGF-beta-induced anterior subcapsular cataract formation. *Am J Pathol.* 2014;184:2001-2012.
  66. Espinoza JA, Gonzalez PA, Kalergis AM. Modulation of antiviral immunity by heme oxygenase-1. *Am J Pathol.* 2017;187:487-493.
  67. Rosetti F, Mayadas TN. The many faces of Mac-1 in autoimmune disease. *Immunol Rev.* 2016;269:175-193.
  68. Lee PY, Wang JX, Parisini E, Dascher CC, Nigrovic PA. Ly6 family proteins in neutrophil biology. *J Leukoc Biol.* 2013;94:585-594.
  69. McKnight AJ, Macfarlane AJ, Dri P, Turley L, Willis AC, Gordon S. Molecular cloning of F4/80, a murine macrophage-restricted cell surface glycoprotein with homology to the G-protein-linked transmembrane 7 hormone receptor family. *J Biol Chem.* 1996;271:486-489.
  70. Simirskii VN, Wang Y, Duncan MK. Conditional deletion of beta1-integrin from the developing lens leads to loss of the lens epithelial phenotype. *Dev Biol.* 2007;306:658-668.
  71. Wang Y, Terrell AM, Riggio BA, Anand D, Lachke SA, Duncan MK. Beta1-Integrin deletion from the lens activates cellular stress responses leading to apoptosis and fibrosis. *Invest Ophthalmol Vis Sci.* 2017;58:3896-3922.
  72. Kerkhoff C, Klempt M, Kaever V, Sorg C. The two calcium-binding proteins, S100A8 and S100A9, are involved in the metabolism of arachidonic acid in human neutrophils. *J Biol Chem.* 1999;274:32672-32679.
  73. Byun JY, Youn YS, Lee YJ, Choi YH, Woo SY, Kang JL. Interaction of apoptotic cells with macrophages upregulates COX-2/PGE2 and HGF expression via a positive feedback loop. *Mediators Inflamm.* 2014;2014:463524.
  74. Wormstone IM, Eldred JA. Experimental models for posterior capsule opacification research. *Exp Eye Res.* 2016;142:2-12.
  75. Robertson IB, Rifkin DB. Regulation of the bioavailability of TGF-beta and TGF-beta-related proteins. *Cold Spring Harb Perspect Biol.* 2016;8:a021907.
  76. Brancato SK, Albina JE. Wound macrophages as key regulators of repair: origin, phenotype, and function. *Am J Pathol.* 2011;178:19-25.
  77. Wynn TA, Barron L. Macrophages: master regulators of inflammation and fibrosis. *Semin Liver Dis.* 2010;30:245-257.
  78. Boswell BA, Korol A, West-Mays JA, Musil LS. Dual function of TGFbeta in lens epithelial cell fate: implications for secondary cataract. *Mol Biol Cell.* 2017;28:907-921.
  79. Lovicu FJ, Schulz MW, Hales AM, et al. TGFbeta induces morphological and molecular changes similar to human anterior subcapsular cataract. *Br J Ophthalmol.* 2002;86:220-226.
  80. Chang C. Agonists and antagonists of TGF-beta family ligands. *Cold Spring Harb Perspect Biol.* 2016;8:a021923.
  81. Zampighi GA, Eskandari S, Kreman M. Epithelial organization of the mammalian lens. *Exp Eye Res.* 2000;71:415-435.
  82. Hoang TV, Kumar PK, Sutharzan S, Tsonis PA, Liang C, Robinson ML. Comparative transcriptome analysis of epithelial and fiber cells in newborn mouse lenses with RNA sequencing. *Mol Vis.* 2014;20:1491-1517.
  83. Blixt A, Mahlapuu M, Aitola M, Pelto-Huikko M, Enerback S, Carlsson P. A forkhead gene, FoxE3, is essential for lens epithelial proliferation and closure of the lens vesicle. *Genes Dev.* 2000;14:245-254.
  84. Wang Z, Divanyan A, Jourdeuil F, et al. Vimentin expression is required for the development of EMT-related renal fibrosis following unilateral ureteral obstruction in mice. *Am J Physiol Renal Physiol.* 2018;315:F769-F780.
  85. Finney AC, Funk SD, Green JM, et al. Epha2 expression regulates inflammation and fibroproliferative remodeling in atherosclerosis. *Circulation.* 2017;136:566-582.
  86. Chao CC, Wu PH, Huang HC, et al. Downregulation of miR-199a/b-5p is associated with GCNT2 induction upon epithelial-mesenchymal transition in colon cancer. *FEBS Lett.* 2017;591:1902-1917.
  87. St Laurent G III, Seilheimer B, Tackett M, et al. Deep sequencing transcriptome analysis of murine wound healing: effects of a multicomponent, multitarget natural product therapy-Tr14. *Front Mol Biosci.* 2017;4:57.
  88. Iglesias-Bartolome R, Uchiyama A, Molinolo AA, et al. Transcriptional signature primes human oral mucosa for rapid wound healing. *Sci Transl Med.* 2018;10:eaap8798.
  89. Nishi O, Nishi K, Imanishi M. Synthesis of interleukin-1 and prostaglandin E2 by lens epithelial cells of human cataracts. *Br J Ophthalmol.* 1992;76:338-341.
  90. Dawes IJ, Duncan G, Wormstone IM. Age-related differences in signaling efficiency of human lens cells underpin differential wound healing response rates following cataract surgery. *Invest Ophthalmol Vis Sci.* 2013;54:333-342.
  91. Findl O, Amon M, Petternel V, Kruger A. Early objective assessment of intraocular inflammation after phacoemulsification cataract surgery. *J Cataract Refract Surg.* 2003;29:2143-2147.
  92. Laurell CG. Inflammatory response after cataract surgery. *Acta Ophthalmol Scand.* 1998;76:632-633.
  93. Butler JM, Unger WG, Grierson I. Recent experimental studies on the blood-aqueous barrier: the anatomical basis of the response to injury. *Eye (Lond).* 1988;(2 suppl):S213-S220.

94. Abbouda A, Tortorella P, Restivo L, Santoro E, De Marco F, La Cava M. Follow-up study of over three years of patients with uveitis after cataract phacoemulsification: outcomes and complications. *Semin Ophthalmol*. 2016;31:532-541.
95. Mohammadpour M, Jafarinasab MR, Javadi MA. Outcomes of acute postoperative inflammation after cataract surgery. *Eur J Ophthalmol*. 2007;17:20-28.
96. Brookshire HL, English RV, Nadelstein B, Weigt AK, Gift BW, Gilger BC. Efficacy of COX-2 inhibitors in controlling inflammation and capsular opacification after phacoemulsification cataract removal. *Vet Ophthalmol*. 2015;18:175-185.
97. Chandler HL, Barden CA, Lu P, Kusewitt DE, Colitz CM. Prevention of posterior capsular opacification through cyclooxygenase-2 inhibition. *Mol Vis*. 2007;13:677-691.
98. Zaczek A, Laurell CG, Zetterstrom C. Posterior capsule opacification after phacoemulsification in patients with postoperative steroidal and nonsteroidal treatment. *J Cataract Refract Surg*. 2004;30:316-320.
99. Lois N, Dawson R, Townend J, et al. Effect of short-term macrophage depletion in the development of posterior capsule opacification in rodents. *Br J Ophthalmol*. 2008;92:1528-1533.
100. Aptel F, Colin C, Kaderli S, et al. Management of postoperative inflammation after cataract and complex ocular surgeries: a systematic review and Delphi survey. *Br J Ophthalmol*. 2017;101:1-10.
101. Sundelin K, Almarzouki N, Soltanpour Y, Petersen A, Zetterberg M. Five-year incidence of Nd:YAG laser capsulotomy and association with in vitro proliferation of lens epithelial cells from individual specimens: a case control study. *BMC Ophthalmol*. 2014;14:116.
102. Wielders LHP, Schouten J, Nuijts R. Prevention of macular edema after cataract surgery. *Curr Opin Ophthalmol*. 2018;29:48-53.